Journal of Membrane Science 726 (2025) 124018



Contents lists available at ScienceDirect

Journal of Membrane Science

journal homepage: www.elsevier.com/locate/memsci



Sustainable ammonia recovery in electrochemical membranes: The critical role of electromigration

Siyao Qi [a], Wen Zhang [b], Guy Z. Ramon [c], Avner Ronen [a,*]

[a] Department of Desalination and Water Treatment, Zuckerberg Institute for Water Research, Jacob Blaustein Institutes for Desert Research, Ben-Gurion University of the Negev, Sede-Boqer Campus, 84990, Israel
[b] Department of Civil and Environmental Engineering, New Jersey Institute of Technology, Newark, NJ, 07102, United States
[c] Department of Civil and Environmental Engineering, Technion-Israel Institute of Technology, Haifa, 32000, Israel

ARTICLE INFO

Keywords:
Electrochemical membrane stripping
Hydrophobic electrically conducting membrane
Ammonia recovery
Electromigration

ABSTRACT

Ammonia (NH_3) is a vital chemical widely used in fertilizers, industry, and as a potential energy carrier. However, conventional ammonia production via the Haber-Bosch process is highly energy-intensive, consuming approximately 13.9 kWh per kg of nitrogen. Additionally, nitrogen-rich wastewater contributes to eutrophication and aquatic toxicity, necessitating sustainable recovery solutions. This study introduces an electrochemical membrane stripping (EMS) system incorporating hydrophobic, electrically conducting membranes (ECMs) to enhance ammonia recovery. By applying a controlled electric field and optimizing cathodic potential and crossflow velocity, the system efficiently transports ammonium (NH_4^+) toward the cathodic membrane, where a localized pH shift converts it into free ammonia (NH_3), eliminating the need for chemical pH adjustment.

Under optimal conditions, the EMS system achieved 88 % ammonia recovery with a high flux of 37 ± 1.45 g m^{-2} d^{-1}, representing a 33.5 % improvement over conventional methods. Mass balance analysis confirmed electromigration as a key transport mechanism, leading to a threefold increase in ammonia concentration at the membrane surface. Additionally, the system demonstrated high energy efficiency, with a specific energy consumption of 2 ± 0.15 kWh per kg of nitrogen, making it a cost-effective alternative for liquid fertilizer production.

As a proof-of-concept, the EMS system was successfully tested on real municipal wastewater, highlighting its practical viability. However, further research is needed to assess long-term stability, scalability, and integration with wastewater treatment infrastructure. This study demonstrates EMS as a promising technology for sustainable nitrogen recovery, supporting circular economy initiatives.

1. Introduction

Ammonia (NH_3) is a widely utilized chemical with key applications in fertilizer production, various industrial processes, and as a potential energy carrier [1,2]. Industrial ammonia production is primarily through the Haber-Bosch process, which converts atmospheric nitrogen into ammonia. However, this process is highly energy-intensive, requiring approximately 13.9 kWh per kilogram of nitrogen, significantly contributing to global carbon emissions [3]. Following its application in various human activities, ammonia is frequently discharged into wastewater, with concentrations typically ranging from 20 to 60 mg L^{-1} in municipal wastewater [4] and up to 3000 mg L^{-1} and higher in anaerobic digestate, landfill leachate or special industrial wastewater [5–7]. The discharge of nitrogen-rich effluents into aquatic environments may result in harmful environmental impacts, including harm to aquatic life and the promotion of eutrophication, which further degrades water quality [8,9].

The primary method for ammonia removal from wastewater is through biological nitrogen removal (BNR) processes, such as nitrification and denitrification. During nitrification, nitrifying bacteria convert ammonia into nitrite and nitrate, which are subsequently converted into atmospheric nitrogen by denitrifying bacteria [9]. However, BNR encounters several challenges, including their reliance on bacterial activity, which is sensitive to factors such as temperature, ammonia concentration, and the presence of other compounds in wastewater. Additionally, BNR can result in the emission of nitrous oxide (N_2O), a

* Corresponding author.
E-mail address: avnerr@bgu.ac.il (A. Ronen).

https://doi.org/10.1016/j.memsci.2025.124018
Received 30 December 2024; Received in revised form 18 March 2025; Accepted 22 March 2025
Available online 27 March 2025
0376-7388/© 2025 The Authors. Published by Elsevier B.V. This is an open access article under the CC BY-NC-ND license (http://creativecommons.org/licenses/by-nc-nd/4.0/).

potent greenhouse gas with a significant global warming potential. Furthermore, BNR is also energy-intensive, requiring approximately 12.5 kWh per kilogram of nitrogen removed [10–12]. Another critical limitation of BNR is the loss of nitrogen species during treatment, as they are generally not recovered for reuse. This shortcoming has driven increasing interest in direct ammonia recovery from wastewater, a more sustainable strategy that promotes nitrogen reutilization and supports circular economy principles [13].

Several methods are available for ammonia recovery, including air stripping, zeolite adsorption, ion exchange, chemical precipitation, and membrane-based processes [14–16]. Each technique presents unique advantages and limitations, influenced by factors such as wastewater composition, recovery efficiency, operational complexity, and energy demand [5]. For instance, air stripping requires the addition of chemicals to adjust the pH to alkaline conditions required to convert ammonium (NH_4^+) into free ammonia (NH_3) for effective removal. This method is also energy-intensive, consuming approximately 23.6–61.1 kWh per kilogram of nitrogen removed [17,18]. Similarly, N recovery through struvite precipitation relies on the addition of magnesium and further pH modification, requiring additional chemical inputs to achieve optimal performance [19]. Membrane stripping has garnered attention as a low-energy alternative for ammonia recovery, with energy consumption typically lower than 1.2 kWh per kilogram of nitrogen [18,20,21]. This approach employs hydrophobic gas-permeable membranes (GPMs), which enable ammonia recovery by allowing ammonia in its gaseous form (NH_3) to pass through the GPM while preventing water from wetting or transport across the membrane. Previous studies have examined the influence of various factors on the efficiency, effectiveness, and selectivity of ammonia removal and recovery. These factors include feed and strip solution characteristics, membrane properties, and operational conditions, all of which play critical roles in optimizing the recovery process [15,17,22]. Among these factors, the feed pH value has been identified as the dominant parameter, significantly impacting the equilibrium of ammonium/ammonia and, thus, the overall recovery efficiency [23]. When the pH of the solution is raised above the logarithmic dissociation constant of ammonia ($pK_a = 9.24$), typically by adding alkaline chemicals (Eq. (1)) [24], ammonium (NH_4^+) is converted into free ammonia (NH_3).

$$NH_4^+ + OH^- \leftrightarrow NH_3 + H_2O \quad \text{[Eq. 1]}$$

Gaseous ammonia diffuses through the hydrophobic GPM due to the partial ammonia pressure difference between the two sides of the membrane [25]. Once diffused, ammonia can be collected through vacuum stripping or by an acidic trap fluid (e.g., sulfuric acid), as described in Eq. (2) [26], forming various liquid ammonium chemicals [27,28].

$$2NH_3 + H_2SO_4 \rightarrow (NH_4)_2SO_4 \quad \text{[Eq. 2]}$$

Membrane stripping has demonstrated notably high energy efficiency for ammonia separation from wastewater [18]. However, this process frequently requires extensive chemical input to increase the pH beyond the ammonium/ammonia equilibrium constant (pK_a). Such pH adjustments contribute substantially to operational expenses and demand large quantities of alkaline chemicals, such as sodium hydroxide or lime. This reliance on chemical addition not only elevates costs but also introduces logistical challenges associated with transporting and storing these substances. These limitations can hinder the practical implementation and scalability of membrane-stripping technology for ammonia recovery, particularly in large-scale or resource-limited settings [29].

In contrast, electrochemical systems generate hydroxide ions (OH^-) at the cathode through water electrolysis (Eq. (3)) [30], which effectively raises the local pH and facilitates the conversion of ammonium to free ammonia (Eq. (1)). Concurrently, an acidic environment can be created near the anode via anodic reactions (Eq. (4)), providing an acidic fluid that is potentially useful for capturing ammonia as it permeates through the **GPM** [31].

$$2H_2O + 2e^- \rightarrow 2OH^- + H_2 \quad [E_0 = -0.42V\ vs.\ SHE] \quad \text{[Eq. 3]}$$

$$H_2O \rightarrow \frac{1}{2}O_2 + 2e^- + 2H^+ \quad [E_0 = +0.82V\ vs.\ SHE] \quad \text{[Eq. 4]}$$

EMS systems commonly incorporate a hydrophobic GPM adjacent to the cathode to enable localized pH adjustment, reduce operational costs without the emission of N_2O, and simplify the logistics of ammonia recovery. Recent advancements have introduced hydrophobic electrically conducting membranes (ECMs), composite polymeric membranes with a thin conductive coating that results in high mass transfer reaction rates due to the shortened diffusion path of free ammonia to the membrane surface [32–34]. As such, ECMs streamline system design and enhance ammonia recovery efficiency as indicated by a 40 % higher ammonium recovery and a high ammonium recovery flux of over 36 g $NH_3 \cdot m^{-2} \cdot d^{-1}$ compared to the configuration of a separated GPM and a metallic cathode. This design achieves approximately 20 % lower energy consumption than conventional systems utilizing a separate GPM and metal cathode [33].

While ECMs in EMS systems have been studied for ammonia recovery, the specific mechanisms governing interfacial mass transport of ammonia, particularly the interplay of local pH gradients and the applied electrical field, remain underexplored [31]. For instance, electromigration facilitates the movement of cationic ammonium from the feed bulk to the negatively charged membrane surface, where it is converted into free ammonia. This localized increase in ammonia concentration at the membrane surface can enhance transport through the membrane, improving overall recovery efficiency. Furthermore, the grafting of carbon nanotubes (CNTs) imparts conductivity to the membrane while simultaneously providing active sites for the preferential sorption of ammonia, thereby enhancing the diffusion of ammonia [35,36]. This functionality may result in a thin accumulation zone for ammonium and ammonia gas at the membrane surface, further promoting efficient ammonia transfer and recovery [37].

This study aims to elucidate the mechanisms driving enhanced ammonia recovery in EMS systems containing ECMs through experimental and theoretical approaches, with a specific focus on the role of electromigration. A novel EMS system featuring a hydrophobic ECM constructed from crosslinked multi-wall CNTs was designed to optimize ammonia recovery by fine-tuning operational parameters such as applied electrical potential and catholyte crossflow velocity. To demonstrate the impact of electromigration, the system's ammonia recovery performance was compared against that of conventional MS systems, which depend on chemical pH adjustment. A mass balance approach was also applied to calculate the free ammonia concentration at the membrane interface, further verifying electromigration's contribution to the ammonia recovery process. Finally, the stability of the system and its ability to strip ammonia was demonstrated using real municipal wastewater.

2. Materials and methods

2.1. Materials

Polytetrafluoroethylene (PTFE) membranes (pore size 0.45 μm) were purchased from Membrane Solutions (China). Carboxyl-functionalized multi-wall carbon nanotubes (CNT-COOH) with a length of 10–30 μm and an outer diameter of 7–8 nm were purchased from Cheap Tubes (USA). Polyvinyl alcohol (PVA, M_w 146000–186000, 99+ % hydrolyzed) and glutaraldehyde (GA) were purchased from Merck (USA). Hydrochloride acid (HCl), sulfuric acid (H_2SO_4), sodium hydroxide (NaOH), and sodium sulfate (Na_2SO_4) were purchased from Bio-Lab, Israel. Ammonium sulfate ($(NH_4)_2SO_4$) was obtained from Sigma-Aldrich (USA). All chemicals were used as received.

2.2. Electrically conducting membrane fabrication and characterization

ECMs were fabricated by spray coating CNT-COOH onto a commercial hydrophobic PTFE membrane as described by Anvari et al. (2020) [38]. Before spraying, the CNT-COOH were dispersed in 99 % ethanol using an ultrasonic tip (VCX130, Sonics &Materials Inc. USA) for 10 min at 50 % intensity. Then, 0.1 wt% PVA and the obtained fresh CNT dispersion were mixed and sprayed onto the pristine PTFE membrane using a lab-scale ultrasonic Spray Coater (NDSP Mini Spray Coater, Nadetech, Spain) at 70 °C. The surface loading of CNT and PVA was 0.5 mg cm^{-2} and 0.0055 mg cm^{-2}, respectively [39,40]. Finally, the CNT layer was stabilized by immersing in a crosslinking solution (11.3 g L^{-1} GA and 4.4 g L^{-1} HCl) at 90 °C for 1 h. After cross-linking, the CNT layer remained intact and adhered well to the ECM surface [41,42]. After rinsing and drying, the obtained ECM was stored at room temperature for further experiments. The morphologies of the pristine PTFE membrane and ECM were examined by a Field Emission Scanning Electron Microscope (FE-SEM, Quanta 200, FEI company, USA) equipped with an Energy Dispersive Spectrometer (EDS; Oxford Instrument, UK). A goniometer (OCA 15 Plus, Data Physics GmbH, Germany) was used to determine the hydrophilicity. The roughness of membranes was measured using Atomic Force Microscopy (AFM, MFP-3D-BIO, Oxford Instruments, US). The gravimetric method was used to estimate the membrane's porosity (Section S1) [39,43]. The electrical resistance of ECM was measured using a four-point probe instrument (Ossila, UK) for at least five distinct 0.5 cm^2 rectangular sections.

2.3. Electrochemical ammonia stripping system configuration

A lab-scale electrochemical membrane stripping (EMS) system with an ECM cathode (surface area of 20 cm^2) was built from transparent polycarbonate (Fig. 1a). An anion exchange membrane (AEM, Fumasep FAS-PET-130, FuMA-Tech, Germany) was used to separate the anode and cathode compartment, each with a 25 mL volume and prevent diffusion of ammonium to the anode.

The synthetic feed solution, formulated to mimic ammonia concentrations in domestic wastewater, contained an ammonia/ammonium-N concentration of 50 ± 2 mg L^{-1}, an electrical conductivity of 1000 ± 100 μS cm^{-1}, and a pH of 6.3 ± 0.3. In addition, the stability and operation of the system were evaluated using real wastewater obtained from a local municipal wastewater treatment facility. The wastewater was filtered to remove particles and bacteria (0.45 μm filter, HAWP04700, Merck, USA) and a total organic carbon (TOC) concentration of 120.1 ± 3.9 mg L^{-1} and an ammonium-nitrogen concentration of 78.6 ± 6.4 mg L^{-1}. The ionic composition, analyzed using coupled plasma-atomic emission spectroscopy (ICP-AES), confirmed the presence of varying ions (e.g., Ca^{2+}, Cl^-, K^+, Mg^{2+}, Na^+, and SO_4^{2-}) with a total electrical conductivity of 1320 ± 58 μS cm^{-1}. Feed solutions were pumped to the cathode compartment (Fig. 1b) using a peristaltic pump (BT100M, Chuangrui, China). The anodic electrolyte, containing 0.01 mol L^{-1} sodium sulfate (Na_2SO_4) solution with a pH of 6.8 ± 0.2, was circulated using a similar peristaltic pump. The stripping solution in the acid tank containing 0.01 mol L^{-1} sulfuric acid with a pH of 1.7 ± 0.2 was continuously circulated in the acid compartment (12.5 mL).

The experiments were performed in chronoamperometry mode using a potentiostat with a three-electrode setup (PalmSense™, Netherlands) under various cathodic voltages, including open circuit potential (OCP), −1.0 V, and −2.5 V (vs. Ag/AgCl), based on prior studies [30], which can impact the electromigration of ammonium cations and modulate the local pH. The ECM (cathode) was used as the working electrode (WE), a porous titanium-plated counter electrode (anode) as the counter electrode (CE), and an Ag/AgCl reference electrode (DRIREF-2SH, World Precision Instruments, US).

2.4. Optimization of ammonia recovery

Initially, optimization experiments were conducted in batch mode by adjusting the applied cathodic potentials without circulation of either the feed or stripping solutions. Batch experiments were conducted for 180 min, and samples were collected from the cathode and acid compartments for further analysis.

Subsequently, experiments were performed in a continuous circulating mode to optimize the crossflow velocity of the feed flow within the cathodic compartment (Fig. 1b), which can influence the boundary layer (bl) thickness near the membrane, thereby enhancing ammonia transport efficiency [44,45]. The cathodic potential was applied at the optimized level determined by the batch experiments. Specifically, 500 mL of the feed solution was circulated at crossflow velocities of 1, 2, and 4 cm min^{-1} between the feed tank and cathodic compartment. The acid stripping solution (200 mL) was circulated at a 10 cm min^{-1} velocity without optimization. Continuous experiments were conducted for 5 h, with samples collected from the feed tank, cathode compartment, and acid tank throughout the operation to measure the NH_4^+/NH_3 concentration and pH. The concentration of NH_4^+/NH_3 was monitored by Nessler's reagent method with a sensitivity of below 1 mg L^{-1}, and the pH was measured using a pH meter (SevenEasy, Mettler-Toledo,

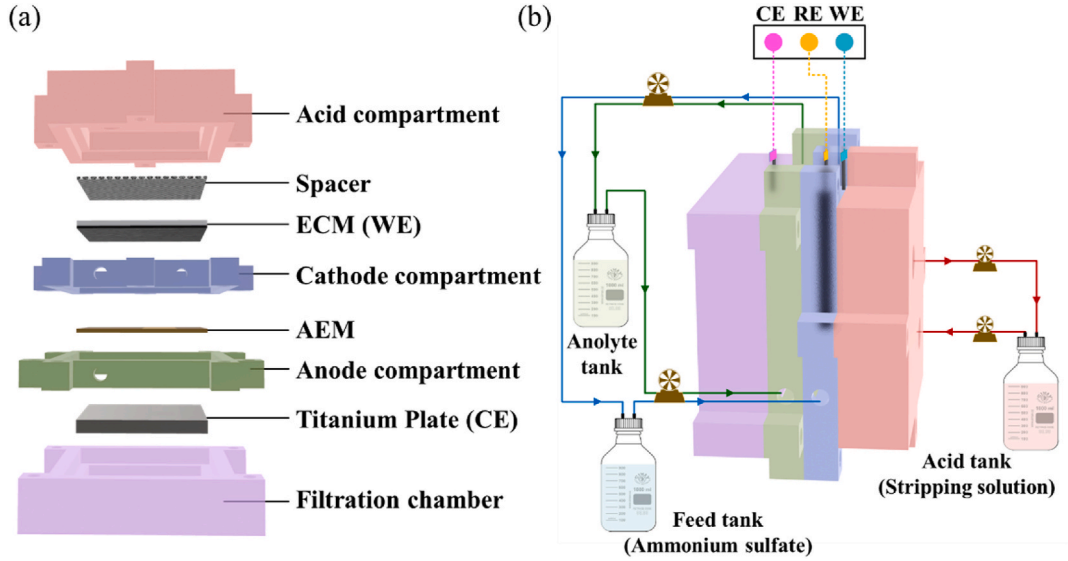


Fig. 1. Schematic illustration of the EMS stripping system. (a) EMS structure and compartments and (b) EMS solutions stream diagram.

Switzerland) [46,47]. Ammonium recovery (%), ammonium flux ($g{\cdot}m^{-2}{\cdot}d^{-1}$), and specific energy consumption ($kWh{\cdot}kg^{-1}$) were calculated using equations detailed in Section S2 (Eqs. S2-S6). These metrics were employed to assess the ammonia recovery efficiency.

2.5. Determination of ammonia recovery mechanism in EMS systems

2.5.1. Experimental setup

The mechanism studies were conducted under an externally applied potential and electric field in a continuous circulating mode in two stages:

Impact of pH Shift: The first set of experiments aimed to determine whether ammonia recovery was solely due to pH shift. Feed solutions with varying initial pH values (6.8, 10, and 12) were circulated in the EMS under OCP conditions. These pH values were selected based on conditions within the cathode compartment (Section 2.4) and estimated pH values near the ECM interface (Section S3) during potentiostatic operation.

Impact of Electromigration: The second set of experiments focused on isolating the role of electromigration from the applied electric field that influences ammonia flux and recovery. These tests were conducted at a cathodic potential of −2.5 V with feed solutions pre-adjusted to a pH of 12. At this high pH, ammonium ions are predominantly present as non-charged free ammonia (as described by Eq. S(15)), minimizing the potential influence of electromigration. Ammonia recovery and flux were then compared to results obtained under a cathodic potential of −2.5 V without pH modification for the feed solution.

All experiments were conducted over 5 h at optimal catholyte crossflow velocities determined in Section 2.4. Samples were collected from the feed tank, cathode compartment, and acid tank at regular intervals during the 5-h operational period for further analysis.

2.5.2. Ammonia transport model

An ammonia transport model was developed to analyze and quantify the mechanisms governing ammonia flux within the EMS system. This model integrates diffusion, electromigration, and pH-dependent equilibrium processes to describe ammonia transport across the ECM. The model assumes steady-state conditions with the feed bulk and stripping solutions considered homogeneous. The transport pathway (illustrated in Fig. 2) follows a sequential mechanism, where ammonia migrates from the feed bulk to the membrane boundary layer (bl) and diffuses through the membrane and into the stripping compartment.

The model employs a mass balance, considering that the flux of ammonia across the membrane, J_m, must equal the combined electromigration and diffusion fluxes. Specifically, on the feed side we employ film theory to sum the difference between the electromigration flux, J_E, which drives ammonium ions toward the membrane under an applied electric field, and the diffusive flux through the boundary layer, J_{bl}, (expressed via a mass transfer coefficient - see details of derivation in the SI S5). The resultant equation is:

$$J_{ov} = \underbrace{K_m \bullet C^G_{NH_3,m}}_{J_m} = \underbrace{V_e \bullet \overline{C_f}}_{J_E} - \underbrace{K_{bl} \bullet \left(C^L_{i,m} - C^L_i\right)}_{J_{bl}} \qquad \text{[Eq. 5]}$$

where K_m is the membrane mass transfer coefficient ($m{\cdot}s^{-1}$), $C^G_{NH_3}$ is the gaseous concentrations of free ammonia at the membrane interface ($mol{\cdot}L^{-1}$), V_e is the electromigration velocity ($m{\cdot}s^{-1}$), $\overline{C_f}$ is the logarithmic mean concentration difference between the bulk and membrane interface (which simplifies the exponential term normally connecting between bulk and membrane concentrations), K_{bl} is the bl mass transport coefficient ($m{\cdot}s^{-1}$), $C^L_{i,m}$ is the aqueous concentrations of species i (ammonia/ammonium) at the membrane interface ($mol{\cdot}L^{-1}$) and C^L_i is the aqueous concentration of species i at the bulk-bl interface ($mol{\cdot}L^{-1}$). Detailed information on each diffusion process is provided in Sections S4-S6, with parameter values used for this study listed in Section S7.

3. Results and discussion

3.1. ECM characterization

SEM images of the pristine PTFE membrane (Fig. 3a) revealed a fibrous morphology attributed to its stretching and annealing treatment. The structure is dominated by large fibers interspersed with numerous smaller, branch-like fibers, resulting in an irregular pore structure (Fig. 3b). Following modification of the membrane by spray coating a CNTs layer as described in Section 2.2, the ECM had a distinctive rough upper surface (Fig. 3d) coated with an intricate network of CNTs (Fig. 3e), consistent with our previous findings [48–50]. SEM-EDS shows

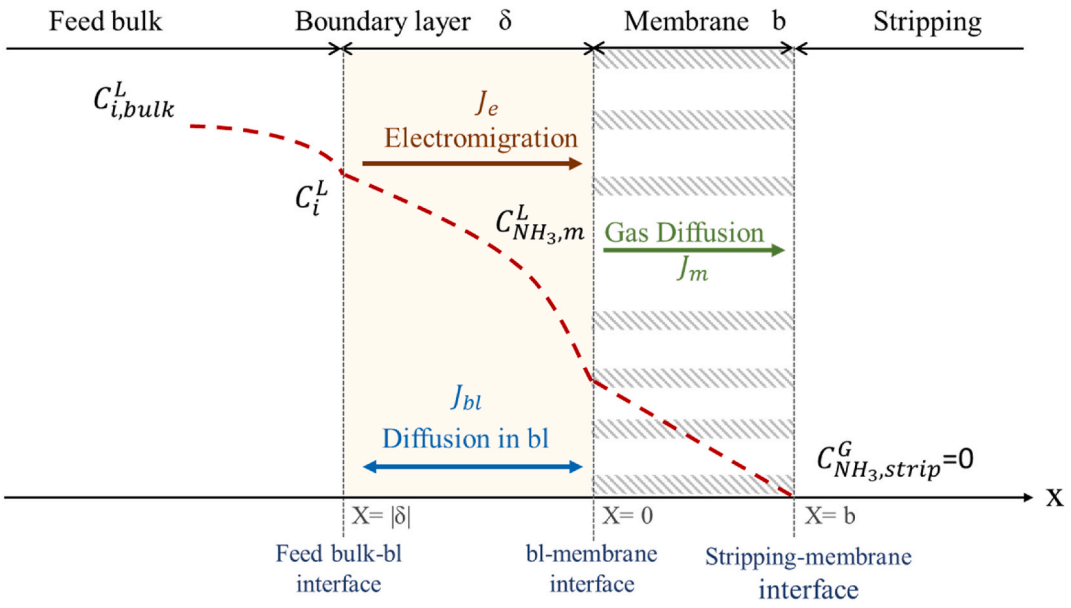


Fig. 2. The schematic representation of ammonia transport pathways highlights the diffusion processes in conventional MS systems and the additional electromigration mechanism in EMS systems. The thicknesses of the boundary layer (δ) and membrane (b) are also indicated (not to scale). The dashed line represents the theoretical ammonia-ammonium concentration gradient across the system.

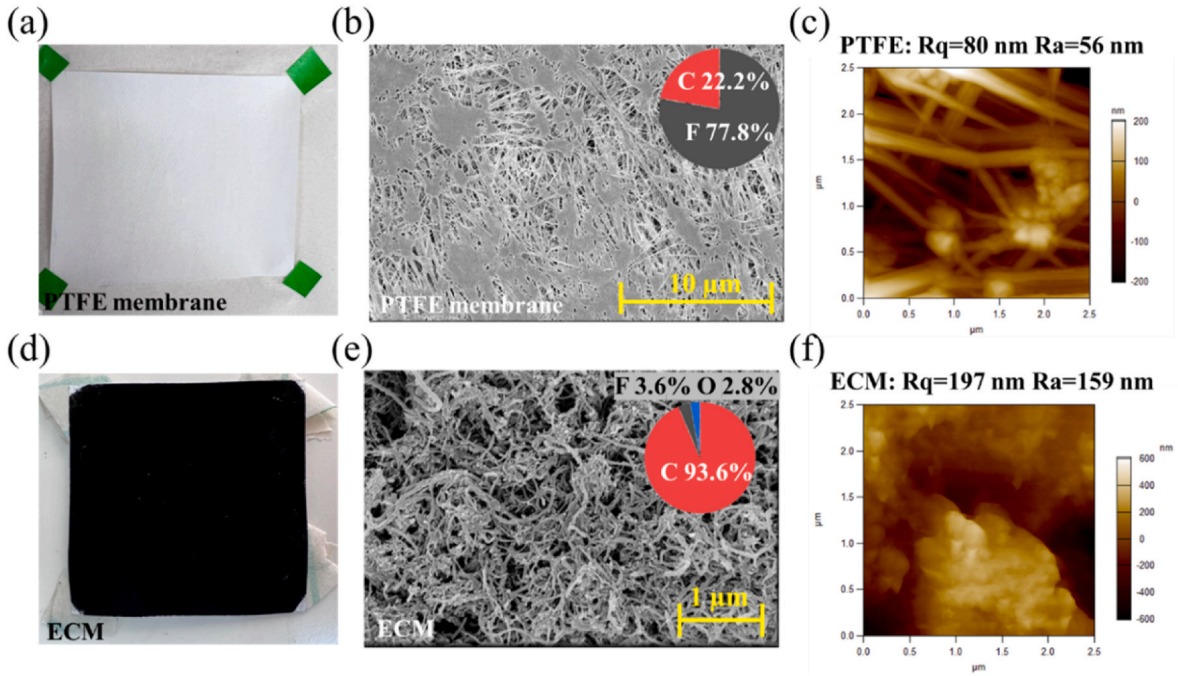


Fig. 3. Characterization of the pristine PTFE membrane and ECM. (a) Image of the pristine PTFE membrane; (b) SEM-EDS analysis of the pristine PTFE membrane, with pie charts illustrating the elemental composition from EDS data; (c) AFM image of the pristine PTFE membrane, showing its surface topology; (d) Image of the ECM coated with CNTs, highlighting the uniform CNT coating; (e) SEM-EDS analysis of the ECM, revealing the elemental composition after coating and (f) AFM image of the ECM, displaying the modified surface structure post-coating.

an increase in the carbon content from 22.2 % for the PTFE membrane to 93.6 % for the ECM resulting from the CNTs coating. AFM imaging (Fig. 3f) revealed that the surface roughness of the ECM increased to 197 nm (compared to 80 nm for the PTFE membrane in Fig. 3c), suggesting that the deposition increased the roughness of the pristine membrane due to the ridge-and-valley characteristic of CNT spray coating [51]. Accordingly, the ECM was slightly more hydrophobic, as indicated by the water contact angles of 129 ± 3.9° and 141 ± 5.4°, for PTFE and ECM, respectively, resulting from the surface roughness and the CNTs layer [39,52–54].

The fabricated ECM demonstrated low electrical resistance, measured at 644.8 Ω·sq^{-1}, and maintained a stable current density of approximately 0, -0.5 and −1.0 A m^{-2} during operation at cathodic potentials of −1.0 and −2.5 V (vs. Ag/AgCl), as shown in Fig. S1. However, further electrochemical characterization using techniques such as cyclic voltammetry and electrochemical impedance spectroscopy was limited due to the hydrophobic nature of the ECM.

3.2. Optimization of ammonia recovery efficiency

3.2.1. Effect of applied cathodic potentials

At OCP, the solution's pH remained constant at 6.5 (Fig. 4a), resulting in a fraction of free ammonia (FA) lower than 1 % (Fig. 4b). This low FA created a limited ammonia concentration gradient between the ECM's feed (and its surface) and the stripping solution, thereby restricting the FA diffusion. As a result, ammonia recovery and flux were relatively low, measuring 0.17 ± 0.02 % (Figs. 4c) and 0.17 ± 0.14 g m^{-2} d^{-1} (Fig. 4d), respectively.

Next, a low cathodic potential of −1.0 V (vs. Ag/AgCl) was applied to the ECM to induce water hydrolysis and promote a pH rise from 6.5 to 8.6 within 60 min in the cathodic compartment (Eq. (3)) [24,48], which stabilized at 9.2 after 120 min (Fig. 4a). As the pH remained slightly below the ammonia-ammonium equilibrium constant, the FA increased to 52 % (Fig. 4b), resulting in a steady rise in ammonium flux, which peaked at 8.01 ± 0.7 g m^{-2} d^{-1} after 60 min. However, the flux declined to 3.44 ± 0.47 g m^{-2} d^{-1} after 180 min due to the gradual depletion of ammonium in the cathode compartment over time. The overall ammonium recovery at these conditions was 47.7 ± 4.5 % after 3 h (Fig. 4c).

Applying a higher cathodic potential of −2.5 V on the ECM resulted in a rapid increase in catholyte pH, reaching 8.96 within 15 min (Fig. 4a) and a higher ammonium flux of 15.65 ± 1.12 g m^{-2} d^{-1} (Fig. 4d) with 17.3 ± 0.72 % ammonium recovery (Fig. 4c). After 30 min and until the end of the experiment, the catholyte pH stabilized at 9.67, corresponding to a FA fraction of 72.76 %. The overall ammonium recovery at these conditions was 77 ± 1.8 %. Additionally, the rapid acid-base reaction between ammonium and sulfate caused a slight increase in the stripping solution's pH, from 1.87 to 2.13 (Fig. S2a). Based on relevant literature, higher cathodic potentials (>2.5 V) were not evaluated as the elevated energy consumption could make the process less efficient economically [31,33]. Further work was done at chronoamperometry conditions of −2.5 V vs. Ag/AgCl reference electrode.

3.2.2. Optimization of catholyte crossflow velocity

The effects of crossflow velocities of 1, 2, and 4 cm min^{-1} were evaluated under a cathodic potential of −2.5 V (vs. Ag/AgCl), as detailed in Section 3.2.1. The flow velocities were chosen to avoid excessive pressure buildup within the experimental setup, which could cause unintended liquid transport through the ECM. As the catholyte crossflow velocity decreased, the extended contact time between the liquid and the membrane led to a higher pH, as shown in Fig. 5a. For all evaluated velocities, the pH remained above the pKa (9.24) for the ammonium-ammonia equilibrium, with measured values of 11.07, 10.4, and 9.53 for crossflow velocities of 1, 2, and 4 cm min^{-1}, respectively. Consequently, at the highest crossflow velocity (4 cm min^{-1}), the FA fraction was 66.10 %, whereas lower crossflow velocities resulted in higher FA fractions of 98.64 % and 93.53 % for 1 and 2 cm min^{-1}, respectively.

Although elevated pH values (above 10) and a high FA fraction at low crossflow velocities were anticipated to result in the highest ammonia recovery [55,56], the maximum recovery was observed at the highest crossflow velocity, reaching approximately 87.63 ± 3.08 %, despite only a limited pH increase (Fig. 5b). Moreover, the ammonium

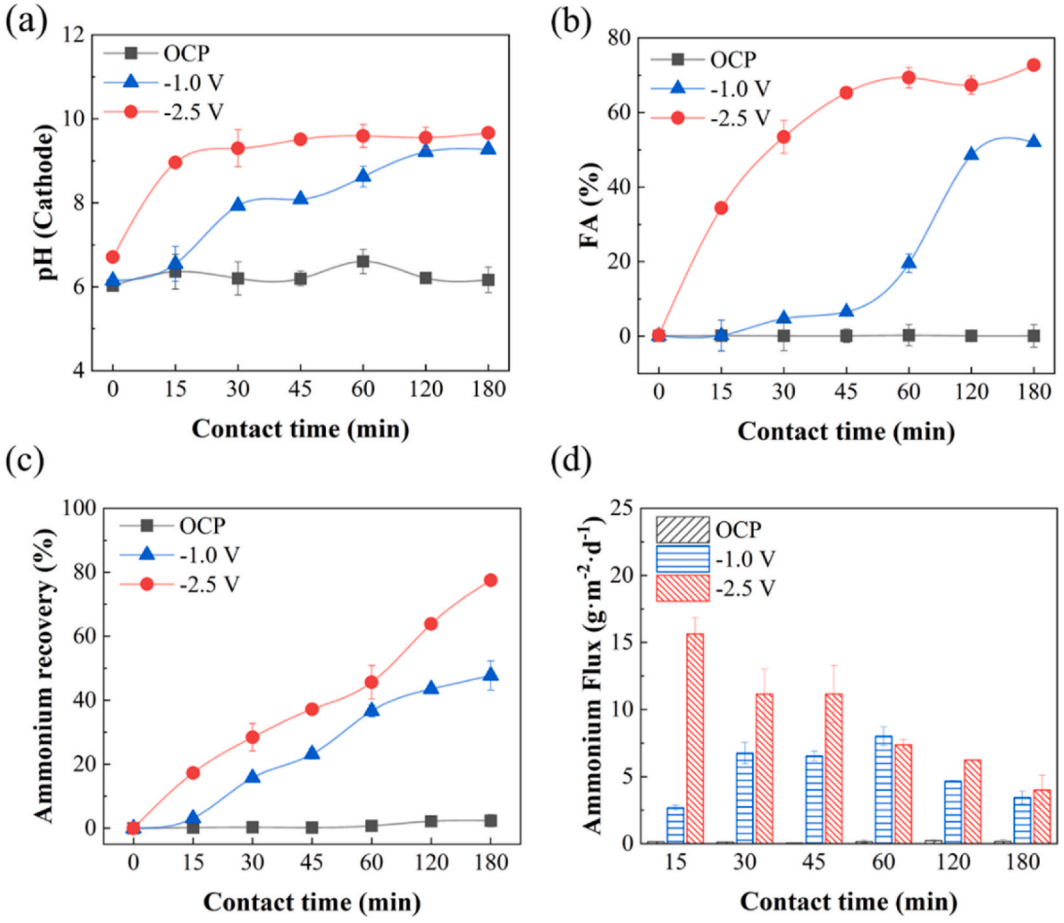


Fig. 4. The performance of ammonia recovery in batch EMS system as a function of applied cathodic potential (OCP, −1.0 V and −2.5 V). (a) Temporal pH changes in the cathodic compartment; (b) Free ammonia fraction; (c) Ammonium recovery rate and (d) Ammonium flux.

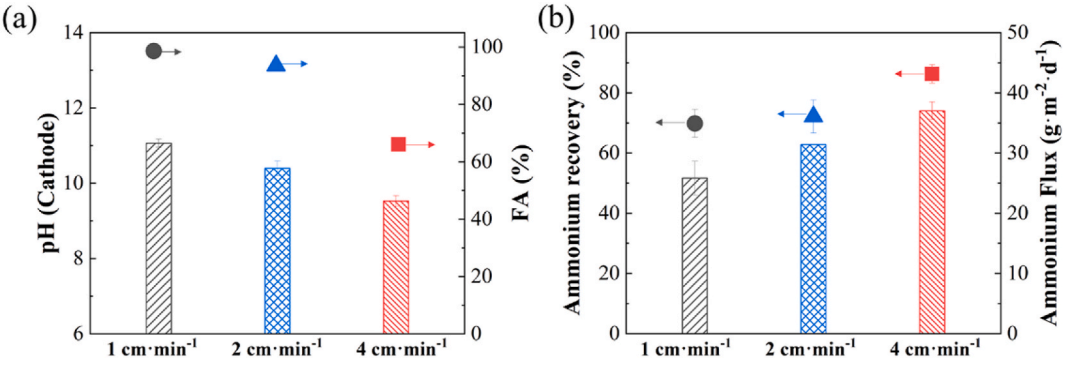


Fig. 5. Performance of ammonia recovery in continuous EMS system at a cathodic potential of −2.5 V (vs. Ag/AgCl) as a function of crossflow velocities (1, 2 and 4 cm min^{-1}) following 5 h of experiments. (a) pH and FA fraction in the cathodic compartment and (b) Ammonia recovery and flux.

flux was highest at this velocity, averaging 37.04 ± 1.45 g m^{-2} d^{-1}, which represented a 30.24 % increase compared to the flux observed at the lowest crossflow velocity (25.85 ± 2.82 g m^{-2} d^{-1}) in Fig. 5b. These results can be attributed to the impact of flow velocity on the mass transport coefficient in the bl [45,55,57]. Calculations of ammonia diffusion across the feed bl (Eqs. S9–S11 in Section S4) revealed that increasing the crossflow velocity from 1 to 4 cm min^{-1} correspondingly enhanced the mass transfer coefficient (K_{bl}) with values of 3.15 × 10^{-6}, 3.96 × 10^{-6} and 4.99 × 10^{-6} m s^{-1}, respectively [45]. These values are consistent with typical K_{bl} values derived from theoretical models and experimental data, which generally range around 10^{-6} m s^{-1} in conventional flat-sheet MS systems under similar laminar crossflow conditions (5 cm min^{-1}) [58]. Overall, the findings indicate that higher crossflow velocities in the cathodic compartment enhance the mass transfer coefficient within the feed bl, promoting greater free ammonia transport to the bl-membrane interface [20,44,45] and improved ammonia recovery.

3.3. Electromigration-driven ammonia recovery enhancement

3.3.1. Experimental results

Experiments were conducted using the conventional MS system at

OCP (influenced solely by the feed pH) and the EMS system at −2.5 V (affected by both the cathode pH and electromigration) under constant ammonium concentration conditions. These tests were carried out using the optimal parameters previously identified. The primary aim was to isolate the specific effects of electromigration and evaluate its direct influence on ammonia recovery.

As illustrated in Fig. 6a, the pH of the feed solution was first adjusted from a neutral baseline (pH = 6.8) to pH 10, simulating the pH conditions observed under a cathodic potential of −2.5 V (Fig. 5a). Subsequently, the pH was further increased to 12 to evaluate the effects of "extreme pH" that may develop near the ECM surface, as calculated in Section S3 [30].

The ammonium recovery performance under these conditions was compared with that of an unmodified feed solution subjected to a cathodic potential of −2.5 V (vs. Ag/AgCl), as shown in Fig. 6b. Under environmental pH conditions (pH~6.8), ammonia recovery was limited to approximately 0.5 ± 1.2 %, primarily due to the low FA fraction of 0.36 % (Fig. 6a). However, when the pH was increased to 10, similar to the catholyte pH observed under an applied potential of −2.5 V, the FA fraction increased significantly to 78.41 %, resulting in an ammonia recovery of 62.52 ± 1.4 %. Further increasing the pH to 12 raised the FA fraction to 99.73 %, yet recovery did not improve, remaining at 58.27 ± 4.28 %. This indicates that at elevated pH levels (greater than 10), the high FA fraction was no longer the limiting factor for ammonia recovery [59,60]. Additionally, ammonium fluxes at pH 10 and 12 were relatively similar, measuring 10.24 ± 1.1 and 9.46 ± 1.18 g m^{-2} d^{-1}, respectively (Fig. 6b). In contrast, when the EMS was operated at −2.5 V, ammonia recovery reached 87.63 ± 3.08 % at pH 10, with an ammonia flux of 37.04 ± 1.45 g m^{-2} d^{-1}. This recovery surpassed the values achieved under chemically modified pH conditions, indicating that the enhanced recovery is not solely attributable to elevated pH. Instead, it highlights the significant contribution of the applied potential and electrical field to the ammonia recovery process.

To further isolate the effects of electromigration, a solution at pH 12 with an applied potential of −2.5 V was compared to a system operated at −2.5 V without prior pH modification. The feed solution predominantly consisted of uncharged ammonia at this high pH, which is not significantly influenced by the electric field or surface charge. The results showed that in the system with both elevated pH and applied potential, the effect of electromigration was limited, as indicated by an ammonia flux of 18.97 ± 1.35 g m^{-2} d^{-1}, only slightly higher than that in the chemically adjusted pH system without applied potential (Fig. 6b). This could be owing to the low percentage of ammonium present in the feed solution at elevated pH, which resulted in insignificant electromigration. Accordingly, this was further supported by the ammonium recovery of 66.15 ± 1.05 % in the system with elevated pH and applied potential, comparable to the recovery of 58.27 ± 4.28 % observed under OCP conditions with chemical pH adjustment (pH = 12). However, these values were notably lower than those achieved in the EMS at −2.5 V without pH modification and containing ammonium ions, where the recovery reached 87.63 ± 3.08 % and the ammonia flux was significantly higher at 37.04 ± 1.45 g m^{-2} d^{-1}. These findings highlight the critical role of the applied potential in driving ammonia recovery, with electromigration playing a more substantial role in enhancing recovery efficiency beyond what can be achieved through pH modification alone.

3.3.2. *Predicted results*

To further clarify the role of electromigration, experimental results were compared with theoretical flux values based on the transport model (Section 2.5.2 and Sections S4-S7). In Fig. 6c, at natural pH, the predicated ammonium flux was approximately 0.115 g m^{-2} d^{-1}, corresponding to the lowest free gaseous ammonia concentration of 5.15 × 10^{-4} mg L^{-1}, while the experimental flux was 0.313 g m^{-2} d^{-1}.

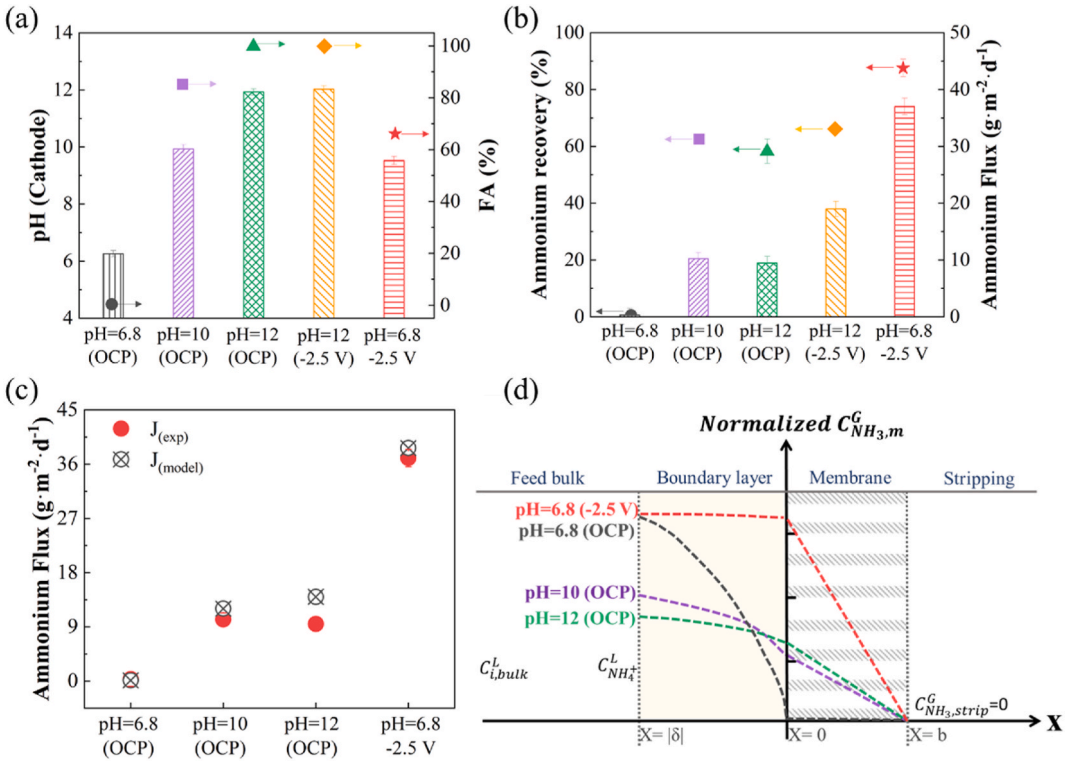


Fig. 6. The performance of ammonia recovery in the membrane stripping system corresponded to pH and applied potential following 5 h of experiments. (a) pH and FA in the cathodic compartment; (b) Experimental ammonium recovery and flux; (c) Comparison of predicted and experimental flux as a function of pH and applied potential and (d) Ammonia transport for the MS and EMS system. The dashed line presents a normalized free gaseous ammonia concentration ($C^G_{NH_3,m}$/ $C^G_{NH_3,m,pH=6.8}$) at the feed bl-membrane interface.

Increasing the pH of the feed solution to 10 resulted in a rise in the predicated ammonium flux to 12.02 g m^{-2} d^{-1}, a 17.4 % difference from the experimental values (10.24 ± 1.1 g m^{-2} d^{-1}), as well in the free gaseous ammonia concentration to 0.0541 mg L^{-1}. At an even higher pH of 12, the free gaseous ammonia concentration at the interface further increased to 0.0628 mg L^{-1}, and the predicated ammonium flux rose to 13.97 g m^{-2} d^{-1} while the experimental flux was 9.46 ± 1.18 g m^{-2} d^{-1}. Overall, the predicated ammonium flux closely aligns with the experimental results, except at a higher pH of 12, which might be attributed to more significant ammonia gas losses in these conditions. Considering the impact of electromigration in the EMS system under an applied cathodic potential of −2.5 V, the predicted ammonium flux was calculated to be 38.68 g m^{-2} d^{-1}. This value was 4.44 % higher than the experimentally observed ammonium flux of 37.04 ± 1.45 g m^{-2} d^{-1}. The close alignment between the predicted and observed flux values reinforces the conclusion that electromigration is essential in driving ammonia recovery within the EMS system. It was mentioned specifically that the free gaseous ammonia concentration at the bl-membrane interface increased to 0.172 mg L^{-1}, an order of magnitude higher than in the MS system (Fig. S3). Free gaseous ammonia concentration at the membrane interface in the MS and EMS system was significantly lower than the initial feed concentration resulting from the mass transfer resistance in the bl, which limits the diffusion of ammonia to the membrane interface and the immediate reaction of ammonia with protons in the stripping solution. This reaction continuously removes ammonia from the interface into the stripping solution, maintaining a low steady-state concentration near the membrane.

In order to clarify the ammonia mass transport process, the predicted normalized free gaseous ammonia concentration (Fig. 6d, dashed line) at the bl-membrane interface was shown, and the concentration of free gaseous ammonia at a pH of 6.8 served as the baseline for normalizing free gaseous ammonia concentration at the membrane interface. When the pH increased to 10, the normalized concentration rose approximately 100-fold, and at a pH of 12, it increased by 122-fold. However, under an applied electric potential of −2.5 V, the normalized concentration further increased by 333-fold, indicating a significant accumulation of gaseous ammonia at the membrane surface, driven by enhanced transport mechanisms facilitated by the electric field.

Overall, in the conventional MS system, the primary driving force for ammonia recovery is the partial pressure difference of free gaseous ammonia across the membrane, with recovery being enhanced by increasing the feed pH. In contrast, the EMS system benefits from electromigration, which concentrates ammonia at the membrane-bl interface [31,61,62]. The applied potential creates a localized elevated pH zone near the membrane surface, promoting the conversion of ammonium to free ammonia and further enhancing recovery.

3.4. EMS stability and ammonia recovery under real wastewater conditions

While the primary objective of this study was to elucidate the role of electromigration in ammonia stripping within EMS systems, assessing the system's long-term stability under challenging conditions is also crucial. To this end, the EMS system was tested using filtered real wastewater obtained from a local municipal wastewater treatment plant. Experiments were conducted over 72 h under the previously optimized conditions (e.g., flow rate and applied potential).

Compared to the synthetic solutions, which reached a pH of 9.53 (Fig. 5), the pH of the real wastewater increased from 7.8 ± 0.2 to 8.8 ± 0.06 within the first 16 h, then stabilized at 8.3 (Fig. 7a). This difference may be attributed to the higher ammonium concentration in wastewater, leading to increased hydroxyl ion consumption, as well as the wastewater's higher buffering capacity.

Despite these variations in pH, ammonium flux remained stable at 36.28 ± 1.03 g m^{-2} d^{-1} (Fig. 7b), which is only slightly lower than the flux observed with synthetic solutions (37.04 ± 1.45 g m^{-2} d^{-1}). These results demonstrate that the EMS system can effectively strip ammonia at a relatively high flux, even under harsh conditions, while maintaining operational stability for longer durations. Furthermore, the ability to sustain high ammonium flux at bulk pH conditions below the ammonium-ammonia pKa suggests that the pH at the membrane's surface is elevated [33] and further supports the electromigration-driven mechanism of ammonia transport.

3.5. Economic assessment of the ammonia recovery using EMS

The energy consumption of the EMS system investigated in this study was compared with that of other MS systems using data from the literature. This comparison is inherently complex due to variability in critical operational parameters, such as bulk ammonium concentration, feed pH, and current density [63], which are not consistently reported across studies (Table 1). The discrepancies in operational conditions can significantly influence energy requirements and system efficiency, making direct comparisons challenging. To standardize the evaluation, energy consumption was calculated based on the applied potential and current per kilogram of nitrogen recovered, excluding costs associated with chemical additives and other operational equipment. This analysis focuses solely on the electrical energy required for ammonia recovery under the specified conditions. While this approach simplifies energy requirements, it may underestimate the total operational costs in a full-scale system, where additional resources and infrastructure are typically involved.

Conventional MS systems using GPM exhibit the lowest energy cost,

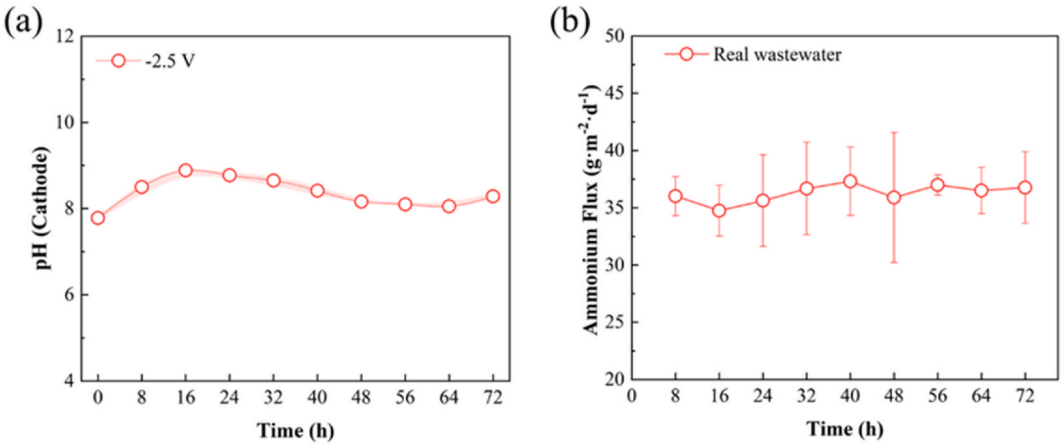


Fig. 7. The performance of the EMS system using real municipal wastewater at a cathodic potential of −2.5 V (vs. Ag/AgCl) (a) pH changes in the cathode compartment and (b) ammonium flux.

Table 1
Comparison of energy consumption and performance metrics for MS and EMS systems.

System	Membrane	Feed concentration ($mg{\cdot}L^{-1}$)	Current density ($A{\cdot}m^{-2}$)	Area (m^2)	Flux ($g{\cdot}m^{-2}{\cdot}d^{-1}$)	Energy ($kWh{\cdot}kg^{-1}$)
MS [64]	PTFE	Digestate (1465–2097)	/	32.3	6.5	0.75
EMS (this work)	CNT-PTFE	SW (60)	1	0.002	37.04 ± 1.5	2.02 ± 0.15
EMS [32]	CNT-PTFE	SW (187)	4.7	0.0044	30.3 ± 6.32	7.0 ± 2.4
EMS [31]	Stainless steel + PTFE	SW (5500)	15	0.0016	208 ± 25	9.7 ± 1.1
EMS [63]	Carbon fiber surface-PP [b]	SW (780)	15.6	0.0032	64.7 ± 5.1	22.05 ± 4.09
EC-MS [66]	ECM with CNT + PTFE	SW (101.3)	40	0.0225	1130	5.87–7.93
EMS [67]	Stainless steel + PTFE	Synthetic urine (6500)	50	0.0064	384 ± 7.7	12.4 ± 0.4

[a] The stripping approach in all MS systems was based on acid-base reactions.
[c] EC-MS = electrocoagulation with electrically conductive membranes system.
[b]PP = polypropylene.

at 0.75 kWh per kilogram of nitrogen recovered [64]. However, this low energy requirement is accompanied by the need for chemical additives to adjust the pH, which can contribute to additional operational costs and environmental considerations [65]. EMS systems have shown a broader range of energy consumption, from 2 to 22 kWh per kilogram of nitrogen, depending on factors such as higher current densities and treatment of solutions with elevated salinity and ammonia concentrations. The EMS system used in this study exhibited an energy consumption of 2.02 kWh per kilogram of nitrogen, representing the lower end of this range. Interestingly, electrochemical membrane stripping processes that use carbon or metal-based PTFE membranes exhibit even higher energy consumption [31,32,34,66,67], approximately 7.0 ± 2.4 kWh per kilogram of nitrogen, despite a similar ammonium flux of 30.3 ± 0.62 g m^{-2} d^{-1} [32]. This increased energy usage may be attributed to distinct electrochemical properties, such as a greater distance between anode and cathode and a stronger electric field, resulting in significantly higher current density (4.7 A m^{-2} compared to 1 A m^{-2} in this study).

Economic cost assessments typically include chemical and operational costs (including the cost of electricity) but exclude labor costs [68]. The chemical cost accounts for the main part of the conventional MS system, while the operational cost represents the primary expense in the EMS system. The cost associated with GPM is low when the feed solution is untreated, and lime is used for pH adjustment [65,69]. Due to scaling issues associated with lime, NaOH is typically preferred, albeit at a higher cost of $4.94 per kilogram of nitrogen, which is significantly lower than that of the EMS system ($7.72 per kilogram of nitrogen) at a current density of 1.56 mA cm^{-2} and the minimum anode area [29,63]. However, at optimal conditions, the operational cost of ammonia recovery in the EMS system was estimated to be much lower, approximately $1.84 per kilogram of nitrogen [68]. This positions the EMS system as a viable alternative to conventional MS systems, particularly in applications where operational efficiency and reduced chemical dependency are prioritized.

Beyond its economic feasibility, EMS technology presents broader environmental and sustainability advantages over conventional ammonia recovery methods. By reducing reliance on chemical pH adjustment, EMS minimizes chemical waste and secondary pollution while simultaneously offering a more controlled and selective recovery process. Additionally, the ability to recover ammonium as a valuable fertilizer (e.g., ammonium sulfate) supports circular economy principles by promoting resource reuse in agricultural applications. Although EMS requires higher initial energy inputs, its long-term benefits, including reduced chemical consumption, lower maintenance costs, and improved ammonia recovery efficiencies, highlight its potential as a sustainable and scalable solution for nitrogen management in wastewater treatment systems.

4. Conclusions

This study demonstrated the potential of EMS systems for efficient ammonia recovery, focusing on the effects of key parameters such as applied potential, pH, and crossflow velocity. Experimental data and theoretical calculations confirmed that EMS can achieve high ammonia recovery by utilizing electromigration and localized electrochemical pH-induced shifts in the ammonium-ammonia equilibrium. Specifically, applying a cathodic potential of −2.5 V and maintaining an elevated pH near the membrane surface significantly enhanced ammonia flux, reaching above 37 ± 1.45 g m^{-2} d^{-1} and achieving recovery efficiencies as high as 87.63 ± 3.08 % under optimal conditions. This performance highlights the ability of EMS to outperform conventional membrane stripping systems, which rely heavily on chemical pH adjustments, by offering a controlled electrochemical approach to ammonia recovery. Theoretical models closely aligned with experimental results at lower pH values, indicating that the model effectively captures the core mechanisms driving ammonia transfer, including electromigration and elevated ammonia concentration at the membrane interface.

Moreover, the system demonstrated stable performance under real wastewater conditions, maintaining a flux of 36.28 ± 1.03 g m^{-2} d^{-1}, only slightly lower than with synthetic solutions, despite the more complex water matrix. While the pH of real wastewater did not reach the levels observed with synthetic solutions, the EMS maintained high ammonia recovery, suggesting that localized pH shifts at the membrane surface and electromigration play a crucial role in facilitating ammonia stripping. These findings highlight the practical viability of EMS for real-world wastewater treatment applications.

The EMS configuration with a CNT-PTFE membrane demonstrated an advantageous balance between energy consumption and recovery efficiency. With an energy consumption of 2.02 ± 0.15 kWh per kilogram of nitrogen, it remains competitive with traditional methods, especially considering the cost savings from reduced chemical inputs.

While the EMS shows promise at the lab scale, further research is necessary to evaluate its scalability and integration with existing wastewater treatment systems. These aspects are crucial for identifying potential challenges in full-scale operations, such as membrane durability, fouling resistance, and energy efficiency over extended periods. Additionally, investigating how EMS can be seamlessly incorporated into current wastewater treatment infrastructures will help pave the way for its broader application and commercialization. Further research into system integration and life cycle assessment (LCA) will be essential in optimizing its environmental footprint and facilitating widespread adoption in industrial and municipal applications.

CRediT authorship contribution statement

Siyao Qi: Writing – review & editing, Writing – original draft, Validation, Methodology, Investigation, Formal analysis, Data curation. **Wen Zhang:** Writing – review & editing. **Guy Z. Ramon:** Writing – original draft, Supervision. **Avner Ronen:** Writing – review & editing, Writing – original draft, Visualization, Validation, Supervision, Project administration, Methodology, Funding acquisition, Formal analysis, Conceptualization.

Declaration of competing interest

The authors declare the following financial interests/personal relationships which may be considered as potential competing interests: Avner Ronen reports financial support was provided by United States-Israel Binational Science Foundation. Wen Zhang reports financial support was provided by National Science Foundation. If there are other authors, they declare that they have no known competing financial interests or personal relationships that could have appeared to influence the work reported in this paper.

Acknowledgment

This work was supported by the NSF-BSF grant (funding #: 2215387 for NSF and funding #: 2022607 for BSF). S.Q. acknowledges the support of the Kreitman School of Advanced Graduate Studies BGU through the Negev fellowship for Ph.D studies.

Appendix A. Supplementary data

Supplementary data to this article can be found online at https://doi.org/10.1016/j.memsci.2025.124018.

Data availability

Data will be made available on request.

References

[1] F. Chang, W. Gao, J. Guo, P. Chen, Emerging materials and methods toward ammonia-based energy storage and conversion, Adv. Mater. 33 (50) (2021) 2005721, https://doi.org/10.1002/adma.202005721.
[2] A.E. Yüzbaşıoğlu, C. Avşar, A.O. Gezerman, The current situation in the use of ammonia as a sustainable energy source and its industrial potential, Curr. Res. Green Sustain. Chem. 5 (2022) 100307, https://doi.org/10.1016/j.crgsc.2022.100307.
[3] Y. Ye, H.H. Ngo, W. Guo, S.W. Chang, D.D. Nguyen, S. Varjani, A. Ding, X.-T. Bui, D.P. Nguyen, Bio-membrane based integrated systems for nitrogen recovery in wastewater treatment: current applications and future perspectives, Chemosphere 265 (2021) 129076, https://doi.org/10.1016/j.chemosphere.2020.129076.
[4] A.M. Schwiebert, J.A. Bush, C. Bellona, J. Vanneste, T.Y. Cath, Membrane contactors for ammonia recovery from anaerobic digester centrate: pretreatment and process optimization, ACS ES&T Water 4 (8) (2024) 3284–3296, https://doi.org/10.1021/acsestwater.4c00162.
[5] T.-L. Chen, L.-H. Chen, Y.J. Lin, C.-P. Yu, H.-w. Ma, P.-C. Chiang, Advanced ammonia nitrogen removal and recovery technology using electrokinetic and stripping process towards a sustainable nitrogen cycle: a review, J. Clean. Prod. 309 (2021) 127369, https://doi.org/10.1016/j.jclepro.2021.127369.
[6] Z. Deng, N. van Linden, E. Guillen, H. Spanjers, J.B. van Lier, Recovery and applications of ammoniacal nitrogen from nitrogen-loaded residual streams: a review, J. Environ. Manag. 295 (2021) 113096, https://doi.org/10.1016/j.jenvman.2021.113096.
[7] Y. Ye, H.H. Ngo, W. Guo, Y. Liu, S.W. Chang, D.D. Nguyen, H. Liang, J. Wang, A critical review on ammonium recovery from wastewater for sustainable wastewater management, Bioresour. Technol. 268 (2018) 749–758, https://doi.org/10.1016/j.biortech.2018.07.111.
[8] J. Zhang, M. Xie, X. Tong, S. Liu, D. Qu, S. Xiao, Recovery of ammonium nitrogen from human urine by an open-loop hollow fiber membrane contactor, Separ. Purif. Technol. 239 (2020) 116579, https://doi.org/10.1016/j.seppur.2020.116579.
[9] D. Gao, T. Xiang, Deammonification process in municipal wastewater treatment: challenges and perspectives, Bioresour. Technol. 320 (2021) 124420, https://doi.org/10.1016/j.biortech.2020.124420.
[10] P.G. Preena, V.J. Rejish Kumar, I.S.B. Singh, Nitrification and denitrification in recirculating aquaculture systems: the processes and players, Rev. Aquacult. 13 (4) (2021) 2053–2075, https://doi.org/10.1111/raq.12558.
[11] Y. Ren, H. Hao Ngo, W. Guo, D. Wang, L. Peng, B.-J. Ni, W. Wei, Y. Liu, New perspectives on microbial communities and biological nitrogen removal processes in wastewater treatment systems, Bioresour. Technol. 297 (2020) 122491, https://doi.org/10.1016/j.biortech.2019.122491.
[12] M. Xie, H.K. Shon, S.R. Gray, M. Elimelech, Membrane-based processes for wastewater nutrient recovery: technology, challenges, and future direction, Water Res. 89 (2016) 210–221, https://doi.org/10.1016/j.watres.2015.11.045.
[13] Y. Ye, H.H. Ngo, W. Guo, S.W. Chang, D.D. Nguyen, X. Zhang, J. Zhang, S. Liang, Nutrient recovery from wastewater: from technology to economy, Bioresour. Technol. Rep. 11 (2020) 100425, https://doi.org/10.1016/j.biteb.2020.100425.
[14] X. Zhang, J. Gu, Y. Liu, Necessity of direct energy and ammonium recovery for carbon neutral municipal wastewater reclamation in an innovative anaerobic MBR-biochar adsorption-reverse osmosis process, Water Res. 211 (2022) 118058, https://doi.org/10.1016/j.watres.2022.118058.
[15] H. Wu, C. Vaneeckhaute, Nutrient recovery from wastewater: a review on the integrated Physicochemical technologies of ammonia stripping, adsorption and struvite precipitation, Chem. Eng. J. 433 (2022) 133664, https://doi.org/10.1016/j.cej.2021.133664.
[16] L. Bianchi, K. Kirwan, L. Alibardi, M. Pidou, S.R. Coles, Recovery of ammonia from wastewater through chemical precipitation, J. Therm. Anal. Calorimetry 142 (3) (2020) 1303–1314, https://doi.org/10.1007/s10973-019-09108-5.
[17] A. Palakodeti, S. Azman, B. Rossi, R. Dewil, L. Appels, A critical review of ammonia recovery from anaerobic digestate of organic wastes via stripping, Renew. Sustain. Energy Rev. 143 (2021) 110903, https://doi.org/10.1016/j.rser.2021.110903.
[18] A. Beckinghausen, M. Odlare, E. Thorin, S. Schwede, From removal to recovery: an evaluation of nitrogen recovery techniques from wastewater, Appl. Energy 263 (2020) 114616, https://doi.org/10.1016/j.apenergy.2020.114616.
[19] F. Ulu, M. Kobya, Ammonia removal from wastewater by air stripping and recovery struvite and calcium sulphate precipitations from anesthetic gases manufacturing wastewater, J. Water Process Eng. 38 (2020) 101641, https://doi.org/10.1016/j.jwpe.2020.101641.
[20] W. Lee, S. An, Y. Choi, Ammonia harvesting via membrane gas extraction at moderately alkaline pH: a step toward net-profitable nitrogen recovery from domestic wastewater, Chem. Eng. J. 405 (2021) 126662, https://doi.org/10.1016/j.cej.2020.126662.
[21] C. Chen, Z. Dai, Y. Li, Q. Zeng, Y. Yu, X. Wang, C. Zhang, L. Han, Fouling-free membrane stripping for ammonia recovery from real biogas slurry, Water Res. 229 (2023) 119453, https://doi.org/10.1016/j.watres.2022.119453.
[22] Y. Zhu, H. Chang, Z. Yan, C. Liu, Y. Liang, F. Qu, H. Liang, R.D. Vidic, Review of ammonia recovery and removal from wastewater using hydrophobic membrane distillation and membrane contactor, Separ. Purif. Technol. 328 (2024) 125094, https://doi.org/10.1016/j.seppur.2023.125094.
[23] D. Qu, D. Sun, H. Wang, Y. Yun, Experimental study of ammonia removal from water by modified direct contact membrane distillation, Desalination 326 (2013) 135–140, https://doi.org/10.1016/j.desal.2013.07.021.
[24] M.E.R. Christiaens, K.M. Udert, J.B.A. Arends, S. Huysman, L. Vanhaecke, E. McAdam, K. Rabaey, Membrane stripping enables effective electrochemical ammonia recovery from urine while retaining microorganisms and micropollutants, Water Res. 150 (2019) 349–357, https://doi.org/10.1016/j.watres.2018.11.072.
[25] G. Lee, K. Kim, J. Chung, J.-I. Han, Electrochemical ammonia accumulation and recovery from ammonia-rich livestock wastewater, Chemosphere 270 (2021) 128631, https://doi.org/10.1016/j.chemosphere.2020.128631.
[26] R.A. Al-Juboori, J. Uzkurt Kaljunen, I. Righetto, A. Mikola, Membrane contactor onsite piloting for nutrient recovery from mesophilic digester reject water: the effect of process conditions and pre-treatment options, Separ. Purif. Technol. 303 (2022) 122250, https://doi.org/10.1016/j.seppur.2022.122250.
[27] X. Vecino, M. Reig, B. Bhushan, O. Gibert, C. Valderrama, J.L. Cortina, Liquid fertilizer production by ammonia recovery from treated ammonia-rich regenerated streams using liquid-liquid membrane contactors, Chem. Eng. J. 360 (2019) 890–899, https://doi.org/10.1016/j.cej.2018.12.004.
[28] L. Cao, J. Wang, T. Zhou, Z. Li, S. Xiang, F. Xu, R. Ruan, Y. Liu, Evaluation of ammonia recovery from swine wastewater via a innovative spraying technology, Bioresour. Technol. 272 (2019) 235–240, https://doi.org/10.1016/j.biortech.2018.10.021.
[29] I. Gonzalez-Salgado, C. Guigui, M. Sperandio, Transmembrane chemical absorption technology for ammonia recovery from wastewater: a critical review, Chem. Eng. J. 444 (2022) 136491, https://doi.org/10.1016/j.cej.2022.136491.
[30] K.M. Kekre, A. Anvari, K. Kahn, Y. Yao, A. Ronen, Reactive electrically conducting membranes for phosphorus recovery from livestock wastewater effluents, J. Environ. Manag. 282 (2021) 111432, https://doi.org/10.1016/j.jenvman.2020.111432.
[31] Z. Wang, J. Zhang, Z. Zhang, Q. Zhang, B. Deng, N. Zhang, Z. Cao, G. Wei, S. Xia, Gas permeable membrane electrode assembly with in situ utilization of authigenic acid and base for transmembrane electro-chemisorption to enhance ammonia recovery from wastewater, Water Res. 258 (2024) 121655, https://doi.org/10.1016/j.watres.2024.121655.
[32] A. Iddya, D. Hou, C.M. Khor, Z. Ren, J. Tester, R. Posmanik, A. Gross, D. Jassby, Efficient ammonia recovery from wastewater using electrically conducting gas stripping membranes, Environ. Sci. Nano 7 (6) (2020) 1759–1771, https://doi.org/10.1039/C9EN01303B.
[33] D. Hou, A. Iddya, X. Chen, M. Wang, W. Zhang, Y. Ding, D. Jassby, Z.J. Ren, Nickel-based membrane electrodes enable high-rate electrochemical ammonia recovery, Environ. Sci. Technol. 52 (15) (2018) 8930–8938, https://doi.org/10.1021/acs.est.8b01349.
[34] J. Zhu, Q. Zhao, J. Wang, N. Li, M. Chen, X. Wang, Negative-pressure gas-diffusion electrode for effective ammonia recovery in bioelectrochemical systems, J. Clean. Prod. 414 (2023) 137641, https://doi.org/10.1016/j.jclepro.2023.137641.
[35] X. Feng, S. Irle, H. Witek, K. Morokuma, R. Vidic, E. Borguet, Sensitivity of ammonia interaction with single-walled carbon nanotube bundles to the presence of defect sites and functionalities, J. Am. Chem. Soc. 127 (30) (2005) 10533–10538, https://doi.org/10.1021/ja042998u.
[36] W. Intrchom, S. Roy, S. Mitra, Functionalized carbon nanotube immobilized membrane for low temperature ammonia removal via membrane distillation, Separ. Purif. Technol. 235 (2020) 116188, https://doi.org/10.1016/j.seppur.2019.116188.
[37] J. Gao, Q. Ma, Y. Zhang, S. Xue, J. Young, M. Zhao, Z.J. Ren, J.-H. Kim, W. Zhang, Coupling curvature and hydrophobicity: a counterintuitive strategy for efficient

electroreduction of nitrate into ammonia, ACS Nano 18 (14) (2024) 10302–10311, https://doi.org/10.1021/acsnano.4c02020.
[38] A. Anvari, K.M. Kekre, A. Ronen, Scaling mitigation in radio-frequency induction heated membrane distillation, J. Membr. Sci. 600 (2020) 117859, https://doi.org/10.1016/j.memsci.2020.117859.
[39] B. Xie, G. Xu, Y. Jia, L. Gu, Q. Wang, N. Mushtaq, B. Cheng, Y. Hu, Engineering carbon nanotubes enhanced hydrophobic membranes with high performance in membrane distillation by spray coating, J. Membr. Sci. 625 (2021) 118978, https://doi.org/10.1016/j.memsci.2020.118978.
[40] M. Han, T. Dong, D. Hou, J. Yao, L. Han, Carbon nanotube based Janus composite membrane of oil fouling resistance for direct contact membrane distillation, J. Membr. Sci. 607 (2020) 118078, https://doi.org/10.1016/j.memsci.2020.118078.
[41] M.A. Halali, M. Larocque, C.-F. de Lannoy, Investigating the stability of electrically conductive membranes, J. Membr. Sci. 627 (2021) 119181, https://doi.org/10.1016/j.memsci.2021.119181.
[42] M. Han, Y. Wang, J. Yao, C. Liu, J.W. Chew, Y. Wang, Y. Dong, L. Han, Electrically conductive hydrophobic membrane cathode for membrane distillation with super anti-oil-fouling capability: performance and mechanism, Desalination 516 (2021) 115199, https://doi.org/10.1016/j.desal.2021.115199.
[43] J. Zheng, Q. Zhang, X. He, M. Gao, X. Ma, G. Li, Nanocomposites of carbon nanotube (CNTs)/CuO with high sensitivity to organic volatiles at room temperature, Procedia Eng. 36 (2012) 235–245, https://doi.org/10.1016/j.proeng.2012.03.036.
[44] J. Park, Y. Jang, W. Lee, Y. Choi, Effect of chemical speciation in boundary layer on performance of ammonia recovery in membrane contactor, Desalination 558 (2023) 116618, https://doi.org/10.1016/j.desal.2023.116618.
[45] H. Liu, J. Wang, Separation of ammonia from radioactive wastewater by hydrophobic membrane contactor, Prog. Nucl. Energy 86 (2016) 97–102, https://doi.org/10.1016/j.pnucene.2015.10.011.
[46] X. Zhao, Q. Geng, F. Dong, K. Zhao, S. Chen, H. Yu, X. Quan, Boosting the selectivity and efficiency of nitrate reduction to ammonia with a single-atom Cu electrocatalyst, Chem. Eng. J. 466 (2023) 143314, https://doi.org/10.1016/j.cej.2023.143314.
[47] Q. Liu, J. Yuan, Z. Gan, C. Liu, J. Li, Y. Liang, R. Chen, Photocatalytic N2 reduction: uncertainties in the determination of ammonia production, ACS Sustain. Chem. Eng. 9 (1) (2021) 560–568, https://doi.org/10.1021/acssuschemeng.0c08064.
[48] S. Qi, A.D. Grossman, A. Ronen, R. Bernstein, Low-biofouling anaerobic electro-conductive membrane bioreactor: the role of pH changes in bacterial inactivation and biofouling mitigation, J. Membr. Sci. 662 (2022) 120960, https://doi.org/10.1016/j.memsci.2022.120960.
[49] Z. Cheng, S. Qi, M. Yang, R. Ben Efraim, H. Yuan, W. Zhang, R. Bernstein, A. Ronen, Advanced tertiary wastewater treatment for enhanced effluent quality by electrically conducting membranes operated at altered potential for simultaneous mitigation of scaling and biofouling, ACS ES&T Eng. 4 (8) (2024) 1902–1913, https://doi.org/10.1021/acsestengg.4c00126.
[50] A. Dan Grossman, S. Qi, A. Aregawi Gebretsadkan, O. Euni Beyioku, T. Turkeltaub, A.I. Shames, Y. Oren, A. Ronen, R. Bernstein, Mechanism of mitigating organic fouling on an electro-conductive membrane under anaerobic conditions and cathodic operation, Appl. Surf. Sci. 654 (2024) 159473, https://doi.org/10.1016/j.apsusc.2024.159473.
[51] M. Lou, X. Zhu, X. Fang, Y. Liu, F. Li, Interception of volatile organic compounds through CNT electrochemistry of electrified membrane surface during membrane distillation, Separ. Purif. Technol. 297 (2022) 121380, https://doi.org/10.1016/j.seppur.2022.121380.
[52] M. Bhadra, S. Roy, S. Mitra, Flux enhancement in direct contact membrane distillation by implementing carbon nanotube immobilized PTFE membrane, Separ. Purif. Technol. 161 (2016) 136–143, https://doi.org/10.1016/j.seppur.2016.01.046.
[53] A. Ashraf, H. Salih, S. Nam, S.A. Dastgheib, Robust carbon nanotube membranes directly grown on Hastelloy substrates and their potential application for membrane distillation, Carbon 106 (2016) 243–251, https://doi.org/10.1016/j.carbon.2016.05.016.
[54] S.M. Lößlein, F. Mücklich, P.G. Grützmacher, Topography versus chemistry – how can we control surface wetting? J. Colloid Interface Sci. 609 (2022) 645–656, https://doi.org/10.1016/j.jcis.2021.11.071.
[55] S.N. Ashrafizadeh, Z. Khorasani, Ammonia removal from aqueous solutions using hollow-fiber membrane contactors, Chem. Eng. J. 162 (1) (2010) 242–249, https://doi.org/10.1016/j.cej.2010.05.036.
[56] Z. Zhu, Z. Hao, Z. Shen, J. Chen, Modified modeling of the effect of pH and viscosity on the mass transfer in hydrophobic hollow fiber membrane contactors, J. Membr. Sci. 250 (1) (2005) 269–276, https://doi.org/10.1016/j.memsci.2004.10.031.
[57] S. Yu, Y. Qin, Q. Zhao, M. Li, H. Yu, G. Kang, Y. Cao, Nafion-PTFE hollow fiber composite membranes for ammonia removal and recovery using an aqueous-organic membrane contactor, Separ. Purif. Technol. 271 (2021) 118856, https://doi.org/10.1016/j.seppur.2021.118856.
[58] A. Hasanoğlu, J. Romero, B. Pérez, A. Plaza, Ammonia removal from wastewater streams through membrane contactors: experimental and theoretical analysis of operation parameters and configuration, Chem. Eng. J. 160 (2) (2010) 530–537, https://doi.org/10.1016/j.cej.2010.03.064.
[59] W. Rongwong, S. Sairiam, A modeling study on the effects of pH and partial wetting on the removal of ammonia nitrogen from wastewater by membrane contactors, J. Environ. Chem. Eng. 8 (5) (2020) 104240, https://doi.org/10.1016/j.jece.2020.104240.
[60] S. Guštin, R. Marinšek-Logar, Effect of pH, temperature and air flow rate on the continuous ammonia stripping of the anaerobic digestion effluent, Process Saf. Environ. Prot. 89 (1) (2011) 61–66, https://doi.org/10.1016/j.psep.2010.11.001.
[61] S.F. Kuchena, Y. Wang, Superior polyaniline cathode material with enhanced capacity for ammonium ion storage, ACS Appl. Energy Mater. 3 (12) (2020) 11690–11698, https://doi.org/10.1021/acsaem.0c01791.
[62] P.P. Kywe, C. Ratanatamskul, Influences of permeate solution and feed pH on enhancement of ammonia recovery from wastewater by negatively charged PTFE membranes in direct contact membrane distillation operation, ACS Omega 7 (31) (2022) 27722–27733, https://doi.org/10.1021/acsomega.2c03673.
[63] X. Wang, S. Im, B. Jung, J. Wu, A. Iddya, Q.-R.A. Javier, M. Xiao, S. Ma, S. Lu, B. Jaewon, J. Zhang, Z.J. Ren, C.T. Maravelias, E.M.V. Hoek, D. Jassby, Simple and low-cost electroactive membranes for ammonia recovery, Environ. Sci. Technol. 57 (25) (2023) 9405–9415, https://doi.org/10.1021/acs.est.3c01470.
[64] P.J. Dube, M.B. Vanotti, A.A. Szogi, M.C. García-González, Enhancing recovery of ammonia from swine manure anaerobic digester effluent using gas-permeable membrane technology, Waste Manag. 49 (2016) 372–377, https://doi.org/10.1016/j.wasman.2015.12.011.
[65] D. Yang, Q. Chen, R. Liu, L. Song, Y. Zhang, X. Dai, Ammonia recovery from anaerobic digestate: state of the art, challenges and prospects, Bioresour. Technol. 363 (2022) 127957, https://doi.org/10.1016/j.biortech.2022.127957.
[66] L. Xu, S. Liu, S. Zhao, K. Li, A. Cao, J. Wang, A novel electrocoagulation-membrane stripping hybrid system for simultaneous ammonia recovery and contaminant removal, Separ. Purif. Technol. 296 (2022) 121377, https://doi.org/10.1016/j.seppur.2022.121377.
[67] A.K. Luther, J. Desloover, D.E. Fennell, K. Rabaey, Electrochemically driven extraction and recovery of ammonia from human urine, Water Res. 87 (2015) 367–377, https://doi.org/10.1016/j.watres.2015.09.041.
[68] Z. Wang, Z. Zhang, J. Zhang, L. She, P. Xiang, S. Xia, Concurrent recovery of ammonia and phosphate by an electrochemical nutrients recovery system with authigenic acid and base, Chem. Eng. J. 454 (2023) 140169, https://doi.org/10.1016/j.cej.2022.140169.
[69] B. Pandey, L. Chen, Technologies to recover nitrogen from livestock manure - a review, Sci. Total Environ. 784 (2021) 147098, https://doi.org/10.1016/j.scitotenv.2021.147098.